Research Article

Graphene Oxide Nanoparticles: A Genotoxic Risk for Patients with Lung Cancer, COPD and Asthma

Emmanuel Eni Amadi

School of Chemistry and Bioscience, Faculty of Life Sciences, University of Bradford, Bradford, West Yorkshire, BD7 1DP, UK.

Abstract

The use of graphene oxide (GO) nanomaterials (NMs) has grown significantly over the last few decades because of their biomedical uses in anti-cancer medication delivery. Because of their distinct physicochemical characteristics and favorable surface chemistry, which includes unbound surface functional groups that facilitate covalent bonding with organic molecules like DNA and RNA, GO NMs are great options for drug delivery nanocarriers. There are worries regarding their genotoxicity despite their growing use in biomedical applications. The impact of GO NMs on DNA has been the subject of relatively few published studies on humans, much less those with chronic lung diseases. The effects of commercial GO (15–20 sheets; 4–10% edge-oxidized; 1 mg/ml) in vitro are examined for the first time in this study. Specifically, DNA damage and other genotoxic endpoints are examined in whole blood and peripheral blood leucocytes (PBL) from both healthy individuals and patients with chronic pulmonary diseases, such as lung cancer, asthma, and chronic obstructive pulmonary disease (COPD). Following thorough characterization of commercial GO NMs, neutral red uptake (NRU) and dimethyl thiazolyl diphenyltetrazolium bromide (MTT) assays were used to perform cytotoxicity studies.. On the other hand, alkaline Comet and cytokinesis-blocked micronucleus (CBMN) assays were used to investigate genotoxicity (DNA damage and chromosome aberration parameters). According to our findings, cytotoxicity, genotoxicity, and chromosome abnormalities increased with concentration, and PBL from patients with lung cancer and COPD was more vulnerable to DNA damage than that of asthma patients and healthy controls. When designed to deliver drug payloads to cells for the treatment of cancer or COPD, GO NMs may play promising roles in drug delivery applications. However, the fact that exposed cells from healthy individuals had higher levels of cytotoxicity, genotoxicity, and chromosome instability parameters all biomarkers of cancer risk should raise concerns about public health, particularly when GO NMs are used as drug delivery nano-carriers in medical treatments and occupational exposures.

Keywords: Graphene Oxide, asthma, chronic obstructive pulmonary disease, lung cancer, MTT assay, Neutral Red Uptake Assay, Micronucleus assay and Comet Assay

Introduction

Because GO NMs can be used as a drug delivery platform to treat a number of chronic diseases, their use has grown dramatically. The two-dimensional planar structure, high surface area-to-volume ratio of 2,600 m2/g (Liu et al. 2013; Wu et al. 2015), surface chemistry of 4–10% edge-oxidization, and heavily unbound surface functional groups like hydroxy -OH, carboxyl/ketone -C=O, epoxy/alkoxy -C=O, and aromatic -C=C groups (Wang et al. 2011b; Mohamadi and Hamidi 2017) are the characteristics that set GO apart from other nanomaterials. Covalent bonding with biocompatible polymers like chitosan, polyethylene glycol (PEG) (Wu et al. 2015), and organic molecules is made possible by their special surface chemistry. (e.g. proteins, RNA, DNA, and drugs) making GO NMs excellent nanocarriers for drug delivery (Rebuttini et al. 2015).

Proteins, small drug molecules, antibodies, and DNA are among the therapeutic agents that have been delivered via GO NMs (Parveen et al. 2012). Numerous medications can be loaded into the structure of a single layer of nano-graphene sheets (NGS) due to its large specific surface area (Sun et al. 2008). A doxorubicin payload is covalently bound to the surface of modified graphene sheets and subsequently released by glutathione, as Zhao and colleagues recently showed (Zhao

**Correspondence*
Emmanuel Eni Amadi
School of Chemistry and Bioscience, Faculty of Life Sciences, University of Bradford, Bradford, West Yorkshire, BD7 1DP, UK.
E-mail: info@amadiglobal.co.uk

et al. 2015). Additionally, studies employing xenograft tumor mouse models demonstrated that NGS was highly absorbed by tumor cells.(Yang et al. 2010). The structural design, drug loading capacity, blood biocompatibility, and the effectiveness of drug release at the appropriate tumor site are some of the factors that have been found to affect the efficacy of GO-based drug delivery systems (Wang et al. 2011a; Liu et al. 2013). The surface of GO NMs can be conjugated with ligands like folic acid (Nasongkla et al. 2004), transferrin receptors (TfR) (Daniels et al. 2006), and polyclonal antibodies specific to particular tumor cells (Dinauer et al. 2005) to increase the specificity of nanocarriers.

In this study, we aimed to evaluate the DNA damage responses (cytotoxicity, genotoxicity, and chromosome instability parameters) after perturbation by GO NMs in human blood samples (whole blood and peripheral blood leukocytes) *in vitro*.

Methodology

Chemicals: Sigma-Aldrich, UK, supplied the following items: graphene oxide 15-20 sheets, 14-10% edge-oxidized, 1 mg/ml dispersion in H2O (Cat. no. 794341); In vitro Toxicology Assay Kit Neutral Red based (Cat. no. Tox-4); bovine serum albumin (BSA; CAS No. 9048-46-8); ethidium bromide (CAS no: 1239-45-8); hydrogen peroxide (30% w/w; CAS no. 7722-84-1); mitomycin C (CAS no: 50-07-7); dimethyl sulfoxide (DMSO; CAS no. 67-68-5); Rosewell Park Memorial Institute medium 1640 (RPMI-1640: Cat no. R8758); and cytochalasin B (CAS no. 14930-96-2). Follicle bovine serum (FBS), low melting point (LMP) agarose (Cat. no. 16520050), normal melting point (NMP) agarose (Cat. no. 17850), RPMI medium 1640 with GlutaMAXTM (Cat. no. 61870010), and phytohaemagglutinin (PHA) (Cat. no. 10576015); 3-(4,5-dimethylthiazol-2-yl)-2,5-diphenyltetrazolium bromide MTT; CAS no. 298-93-1; Cat. No. M6494) were purchased from Thermo Fisher Scientific, UK. All other chemicals were of analytical grade and were sourced locally.

Nanoparticle Characterisation

Preparation of GO Suspension for Particle Size and Surface Charge Analysis

From the 1 mg/ml stock dispersion to a final volume of 1,000 µl using pure water, four distinct working stock concentrations of GO (10, 20, 50, and 100 µg/ml) were created. Before being used, all working stock suspensions were sonicated for five minutes at 30 W using a Sonics Vibra Cell (Sonics & Materials Inc., New Town, USA).

Dynamic Light Scattering (DLS) and Zeta Potential (ZP) Analysis

Pure water was used to dilute a small amount of each working stock suspension 1:100. The diluted solutions were put into plastic cuvettes for DLS measurements, and a Zetasizer Nano-ZS (Malvern Instruments, UK; Model ZEN3600) was used to measure the particle size distribution in triplicate at room temperature (RT; 25°C). The same Zetasizer Nano-ZS was used to measure the ZP readings for 16 runs at 25°C after the diluted samples were moved into a sterile Zeta cell. To make sure the particles were evenly distributed throughout the suspension, the suspensions were gently stirred before each measurement.

Scanning Electron Microscope (SEM) Analysis

For the SEM analysis, the different working stock suspensions of GO NMs (10, 20, 50 and 100 µg/ml) were allowed to air-dry overnight prior to loading the SEM sample stub onto the sample stage. The stub was then tightened and positioned in place to obtain a better image. The sample stage was then placed inside the sample chamber and the compartment closed and evacuated Using the SEM software. the operating voltage was set to 20.0 kV and the two-dimensional (2-D) SEM images were analysed at 20K magnification (FEI Quanta 400, Cambridge, UK).

Transmission Electron Microscope (TEM) Analysis

A TEM was used to measure the size and aggregation characteristics of the dried GO NMs. Briefly, the different working stock suspensions of GO (10, 20, 50 and 100 µg/ml) were first filtered through carbon-coated copper TEM grids (300 mesh), followed by washing off excess particles from the grids by dipping them 50 x in pure water. The dried grids containing the particles were then evaluated using the TEM (JEM-2100, JEOL Ltd., Tokyo, Japan) at 20.0 kV with various magnifications (50x; 1,000x; and 2,500x) and three-dimensional (3-D) TEM micrographs were obtained.

Blood Sample Collection

A skilled phlebotomist collected blood samples in 5-ml Vacuette® LH lithium heparin-coated tubes following informed consent. The University of Bradford's Research Ethics Sub-Committee had granted ethical approval for human subjects (Reference No.: 0405/8). Additionally, the Research Support and Governance Office of Bradford Teaching Hospitals NHS Foundation (Reference No. DA1202) and the Leeds East Research Ethics Committee (Reference No. 12/YH/0464) reviewed it. Patients with lung cancer, COPD, and asthma were gathered from the clinics of Dr. Abid Aziz, a respiratory consultant at St. Luke's Hospital NHS Trust in Bradford, West Yorkshire, UK, and Professor Badie K. Jacob at Bradford Royal Infirmary. People in good health were chosen from the University of Bradford's student community and volunteers from Blackley, North Manchester, UK. Blood samples were used on the day of collection. Unused blood that remained on the day of collection was diluted with RMPI-1640 1:2 followed by the addition of 10% DMSO. The diluted blood samples were then divided into aliquots and stored in a deep

freezer at -80°C. Only fresh blood samples were used in the cytotoxicity and genotoxicity assays. The demographic data of healthy individuals and patients who participated in the study are shown in **Tables 1-4**

Isolation of Peripheral Blood Leukocytes

With minor adjustments, the Lymphoprep™ density gradient centrifugation method was used to separate peripheral blood leukocytes (PBL) from whole blood from both healthy individuals and patients with lung cancer, COPD, and asthma (Böyum 1968; STEMCELL Technologies 2017). They were transferred into 50 ml Universal tubes prefilled with 10 ml of 0.9% NaCl and then centrifuged at 630 x g for 15 min at room temperature (RT). Leukocyte pellets were resuspended in 700 µl of RPMI-1640 medium after the supernatant was discarded, and a Neubauer hemocytometer was used to count the cells. The cell concentration was calculated, and the final volume of the leukocyte suspension was adjusted for cell culture.

Cytotoxicity assays

MTT and Neutral Red Uptake Assays

The MTT or (3-(4,5-dimethylthiazol-2-yl)-2,5-diphenyltetrazolium bromide) tetrazolium reduction assay, a colorimetric assay that measures the metabolic activity of mitochondria in living cells (Mossman 1983b), and the Neutral Red Uptake assay, which measures the metabolic activity of lysosomes in living cells in the presence of chemical agents, were used to treat isolated PBL from various blood donor groups (see Tables 1-4), i.e. from healthy individuals (11/AM, 12/WJ and 13/AN), asthma patients (18/0809845, 19/PU and 20/TA), COPD patients (18/CX, 19/QC and 20/0290072), and lung cancer patients (198/ZA, 19/4360497856 and 20/0795624). (Sigma-Aldrich USA 2018) - were performed according to the manufacturers' recommended guidelines. Absorbances of the dyes were measured. which are proportional to the number of living cells, was then quantified in triplicate (n = 3) using a spectrophotometer (Multiscan™ FC Microplate reader).

Genotoxicity Assays

Comet Assay

The GO concentrations used to treat diluted whole blood (1:10 in RPMI 1640) were 0.1, 0.2, 0.5, and 1 µg/ml. The amount of GO suspension added was restricted to 1% of the 1 ml treatment volume. While 100 µM hydrogen peroxide (H2O2) was used as a positive control (PC) because it caused significant DNA damage and more than 75% of the cells survived, the RPMI-1640 medium alone was used as the negative control

Table 1: Demographic data of recruited healthy control individuals with no smoking history and no medical history of severe disease. Samples from donors18,19 and 20 were used for cytotoxicity studies.

Sn	Code	Age (Years)	Sex	Ethnicity	Smoking History	Medical History
1.	10335	39	M	Caucasian	None	None
2.	10329	39	F	Caucasian	None	None
3.	10331	69	M	Caucasian	None	None
4.	JW 27-8-15(Box91)	40	M	Caucasian	None	None
5.	23-24(Box 84)	44	F	Caucasian	None	None
6.	No-35-36	56	F	Caucasian	None	None
7.	17-06-15 MA	47	M	Caucasian	None	None
8.	MS 23-06-15	39	M	Caucasian	None	None
9.	10588	32	F	Asian	None	None
10.	10-12-18	47	M	Caucasian	None	None
11.	AM	45	F	Caucasian	None	None
12.	WJ	47	M	Caucasian	None	None
13.	AN	43	M	Caucasian	None	None
14.	HC	56	M	Caucasian	None	None
15.	JH	24	M	Caucasian	None	None
16.	TA	42	F	Caucasian	None	None
17.	PN	39	F	Caucasian	None	None
18	AH	48	M	Caucasian	None	None
19	NA	50	M	Caucasian	None	None
21.	EW	46	F	Caucasian	None	None

Table 2: Demographic data of recruited patients diagnosed with asthma. Samples from donors 18,19 and 20 were used for cytotoxicity studies.

SN	Code	Age (years)	Sex	Ethnicity	Smoking History	Medical History
1.	27-10-15 R	45	M	Caucasian	Smoker,3-5/day	None
2.	21-10-15 R	32	F	Caucasian	Non-smoker	None
3.	13-3-17 R4 0339423	31	F	Asian	Non-smoker	None
4.	13-3-17 R2 0505001	61	M	Caucasian	Smoker; 40/day; 30/year	Asthma & COPD
5.	13-3-17 R3 0538130	54	F	Caucasian	Smoker; 15-20/ day	Asthma & COPD
6.	R 21-10-15	32	F	Caucasian	Non -Smoker	NA
7.	RAE 0144596	47	F	Caucasian	Not recorded	None
8.	9/3/17 R2 RAE 1317552	54	F	Caucasian	Past Smoker	None
9.	R4 13-3-17	64	M	Caucasian	Non -Smoker	None
10.	24/2/17 RAE 0797968	38	F	Caucasian	Not recorded	None
11.	9-3-17	49	M	Caucasian	Smoker; 3/day	None
12.	03-12-18	64	F	Asian	Non -Smoker	None
13.	6-12-18	46	F	Asian	Non -Smoker	None
14.	1182462; 4500698388	61	M	Caucasian	Non -Smoker	None
15.	N/A	65	M	Caucasian	Non -Smoker	None
16.	N/A	58	F	Caucasian	Non -Smoker	None
17.	N/A	60	M	Caucasian	Non -Smoker	None
18.	0809845	26	F	Caucasian	Non -Smoker	None
19.	PU	64	F	Asian	Non -Smoker	None
20.	TA	46	F	Asian	Non- Smoker	None

(NC) (Amadi 2019). Before the alkaline Comet assay (pH >13), which was carried out as previously described (Tice et al. 2000; Karbaschi and Cooke 2014; Azqueta and Dusinska 2015; OECD 2016), incubation was conducted for 30 minutes at 37°C in a cell culture incubator.

Cytokinesis-Blocked Micronucleus (CBMN) Assay

For 30 minutes, RPMI-1640 culture medium with stable glutamine (Life Technologies, UK) was equilibrated to 37°C and 5% CO2. It was then supplemented with 15% foetal bovine serum (FBS; VWR, UK) and 1% penicillin-streptomycin solution (VWR, UK). 400 µl of whole blood, 130 µl of phytohemagglutinin (PHA), and 4.5 ml of the equilibrated basic medium were used to set up cell cultures in a sterile environment. They were gently mixed and then incubated for 24 hours at 37°C with 5% CO2. Cells were treated with 0.1, 0.2, 0.5, and 1 µg/ml GO NMs following a 24-hour incubation period. Only 1% of the 5 ml treatment volume could be added to the GO suspension. RPMI-1640 and 0.4 µM mitomycin C were utilized for the NC and PC. The CBMN assay was carried out as previously described (Fenech 2007). A minimum of 1,000 cells, including mono-, bi-, and multinucleated cells (MonoNC, BiNC, and MultiNC), were scored in order to determine the nuclear division index (NDI) per treatment concentration. Cytogenetic damage was assessed in BiNC by calculating the number of induced micronuclei (MNi), nuclear plasmatic bridges (NPB), and nuclear buds (BUD) per 1,000 BiNC. Additionally, micronuclei in MonoNC were recorded. The experiments were repeated five times (n=5) for each treatment group (healthy, asthma, COPD, and lung cancer groups).

Statistical Analysis

In order to determine differences in cytotoxicity, genotoxicity, and frequencies of cytogenetic parameters (MNi, MonoNC, BiNC, MultiNC, NPBs, and NBUDs) between treated cells (healthy individuals and patients: asthma, COPD, and lung cancer) and untreated, NC samples, statistical analysis was conducted using the GraphPad Prism® software, version 7.04 (Fay Avenue, La Jolla, CA, USA), which was used to express the data as the mean ± SEM. The following criteria were used to determine statistical significance: * $p < 0.05$; ** $p < 0.01$; *** $p < 0.001$; and ns = not significant.

Experiential Results

Nanoparticle Size Distribution / Agglomeration State, and Surface Charge

In this study, the characterization of GO NMs using the Zeta sizer Nano to determine the particle size-distribution and

Table 3: Demographic data of recruited patients diagnosed with COPD. Note: 18, 19 and 20 were used for cytotoxicity studies.

SN	Code	Age (years)	Sex	Ethnicity	Smoking History	Medical History
1.	5-8-15 R2	52	M	Caucasian	Smoker; 20/day	None
2.	09-06-15 R	65	F	Caucasian	Smoker; 5-10/day	None
3.	13-3-17 R2 0505001	61	M	Caucasian	Smoker; 40/day; 30/year	Asthma & COPD
4.	13-3-17 R3 0538130	54	F	Caucasian	Smoker; 15-20/day	Asthma & COPD
5.	13-3-17 R1 1308631	56	F	Caucasian	Past Smoker	None
6.	R 09-06-15	55	M	Caucasian	Smoker; 20-80/day	None
7.	R2 05-08-15	64	M	Caucasian	Smoker	None
8.	R1 27-2-17; RAE 0255865	64	M	Caucasian	Smoker; 20/day	None
9.	R3 27-2-17 DJ1	54	F	Caucasian	Smoker; 6-8/day	None
10.	R3 28-2-17	69	M	Caucasian	Smoker	None
11.	R1 2-3-17 RAE 1165577	64	M	Caucasian	Smoker; 20/day	None
12.	R2 2-3-17 RAE 0716425	70	F	Caucasian	Smoker; 15-20/day for 20 yrs	Severe COPD/ recurrent chest infection
13.	9/3/17 R1 RAE 0292614	49	M	Asian	Smoker; 20/day; Cannabis; pop usually	COPD; Schizophrenia
14.	6-12-18	54	F	Caucasian	Past Smoker; Tobacco	None
15.	3340032	57	M	Caucasian	Smoker	None
16.	367885	59	M	Caucasian	Smoker; 30/day	None
17.	4360497856	57	M	Caucasian	Smoker	None
18.	CX	58	M	Caucasian	Past Smoker	None
19.	QX	54	F	Caucasian	Past Smoker/ tobacco	None
20.	0290072	57	M	Caucasian	Smoker; 30/day; alcohol	None

surface charge in an aqueous solution. The results regarding DLS (dynamic light scattering), TEM and SEM (transmission and scanning electron microscopy) are shown in Table 5. In terms of size distribution, we found that GO NMs were evenly distributed following a mild shake prior to the experiment, but eventually clumped together on the cuvette's base. The polydispersity index (PdI), which gauges the broadness of the particles, was 0.87±0.05; the mean electro-kinetic zeta potential (ZP), or surface charges, was -23±2 mV; and the Z-Average (d.nm) of GO agglomerates with 15–20 layers was 760±31 nm, which indicates that each layer's particle size was 38–51 nm thick. GO NM sheets aggregated in aqueous dispersion due to high inter-particulate forces of attraction (Van der Waal forces), resulting in the formation of massive flakes of GO sheets on top of each other.

Specifically, the TEM micrographs showed enormous lumps of GO sheets densely packed on top of each other in a high agglomeration state: aggregated tiny sheets of GO piled on top of bigger agglomerates all contending for space.

Cytotoxicity and Viability Assessments

NRU (Neutral Red Uptake) and MTT assays

Figure 2 shows a plot of the percentage (%) of cell survival in the NRU and MTT assays against varying GO NM concentrations. A careful examination of the two graphs revealed that GONPs were cytotoxic at lower concentrations of up to 0.2 µg/ml, as indicated by sharp slopes, and that they were highly cytotoxic to PBL at higher concentrations of 0.2 to 1.0 µg/ml, as indicated by the steady declines in the slopes in each treatment group: lung cancer (red), COPD (green), asthma (blue), and healthy people (black).

In the NRU assay (Figure 2A), the % cell survival rates of PBL after treatment with 0.1 µg/ml (healthy individuals) decreased in a non-significant manner from 100% to 93.6%. However, as the GO concentrations increased from 0.1 to 0.2 µg/ml, the % cell survival rates of PBL from healthy individuals decreased sharply to 70.71% ($p < 0.01$), while cells from patient groups showed gradual significant decreases in % cell survival rates to 61.14% (asthma group, $p < 0.001$), 57.01% (COPD group,

Table 4: Demographic data of recruited patients diagnosed with lung cancer. Note: Sections in grey were used for cytotoxicity studies. Note: Samples 18, 19 and 20 from donors were used for cytotoxicity studies.

SN	Code	Age (years)	Sex	Ethnicity	Smoking History	Medical History
1.	5-8-15 R3	64	M	Caucasian	Smoker; 8/ day	None
2.	29-7-15 R	62	M	Caucasian	Smoker; 10-15 day	None
3.	05-08-15 R	62	F	Asian	Non-Smoker	None
4.	06-08-15 R2	74	M	Caucasian	10-15/ day	None
5.	05-08-15 R1	60	F	Asia	Non - Smoker	None
6.	R1 7-12-2016	64	M	Caucasian	Smoker	None
7.	R2 7-12-2016	77	F	Caucasian	Smoker	None
8.	12-1-17	64	M	Caucasian	Smoker	Lung nodule
9.	13-12-18	55	F	Asian	Past Smoker	None
10.	0795624	65	M	Caucasian	Smoker; 30 pack/ year	None
11.	0564145	72	F	Caucasian	Smoker	None
12.	0290072	57	M	Caucasian	Smoker; 30/day	Pulmonary fibrosis; COPD
13.	N/A	60	F	Caucasian	Past Smoker	None
14.	N/A	50	M	Caucasian	Past Smoker	None
15.	N/A	65	M	Asian	Past Smoker	None
16.	N/A	61	F	Caucasian	Past Smoker	None
17.	N/A	68	M	Caucasian	Past Smoker	None
18.	ZA	55	F	Asian	Past Smoker	None
19.	4360497856	57	M	Caucasian	Smoker; 30/day	None
20.	0795624	65	M	Caucasian	30 pack/ year	None

$p < 0.001$), and 49.48% (lung cancer group, $p < 0.01$). These decreases were statistically significant for the asthma, COPD, and lung cancer groups, with the percentage cell survival rates dropping to 67.29% (asthma group, $p < 0.01$), 65.6% (COPD group, $p < 0.05$), and the lowest value of just under 60% (lung cancer group, $p < 0.01$). The percentage of PBL cell survival rates declined significantly ($p < 0.01$) after exposure to 0.5 and 1 µg/ml GO, as indicated by the gradient slopes, to 69.96% and 51.21% in the healthy individual group, to 57.24% and 55.57% in the asthma group, to 46.69 and 38.60% in the COPD group, and to 39.35% and 27.74% in the lung cancer group, respectively. Overall, the percentage of lung cancer leukocytes that survived was the lowest when compared to COPD, asthma, and healthy controls.

In the MTT assay (Figure 2B), the percentage of PBL cells that survived treatment with varying concentrations of GO NMs (0.1, 0.2, 0.5, and 1 µg/ml) decreased. In particular, the percentage of PBL cells that survived treatment with GO NMs between 0.1 and 0.2 µg/ml decreased significantly ($p < 0.01$) in a concentration-dependent manner from 100% to 83.08% and 55.01% in the Healthy Individual Group, to 80.01 % and 61.67% in the asthma group, to 74.99% and 50.03% in the COPD group, and 70.01% and 43.46% in the lung cancer group, respectively, to 44.97% and 40.04% (asthma group), 34.99% and 26.99% (COPD group) and to the lowest values of 29.99% and 20.60% (lung cancer group), respectively.

Overall, the % cell survival rates of leukocytes from lung cancer patients in both NRU and MTT assays were the lowest ($p < 0.001$) when compared to the other treatment groups (COPD, asthma, and healthy controls).

Genotoxicity and DNA Damage

The Comet Assay

The histograms in Figure 3A (OTM) and Figure 3B (% tail DNA) display the Comet assay results for both parameters, OTM and % tail DNA. After 30 minutes of exposure, GO NMs significantly damaged PBL's DNA in a concentration-dependent manner (0.1, 0.2, 0.5, and 1 µg/ml) in comparison to untreated cells. PBL originating from lung cancer patients (lung cancer group) exhibited the highest level of induced DNA damage for both parameters, OTM and % tail DNA, for each GO concentration. The COPD and asthma groups came next. The control group's PBL from healthy people had the

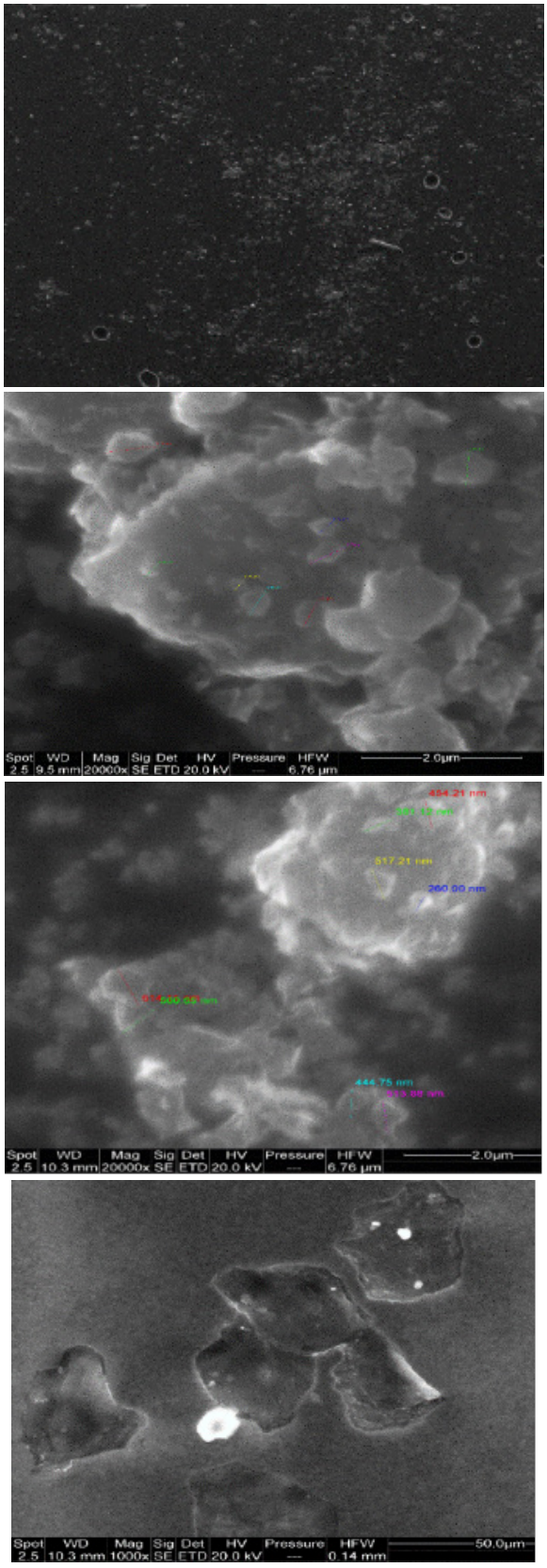

Figure 1: Characterisation of GO NM,15-20 sheets. Micrographs: SEM: (A) = 50x Mag.; Scale Bar: 1.0 mm; TEM: (B): 20,000x mag.; Scale Bar: 2.0 µm; (C): 20,000 mag.; Scale Bar: 2.0 µm, respectively.

least amount of DNA damage. Notably even for the lowest concentration of 0.1 µg/ml, DNA damage (% tail DNA) in PBL was found to be significantly ($p < 0.001$) higher for the lung cancer group, followed by the asthma and COPD groups. A closer observation of the untreated PBL of the negative control showed basal DNA damage for all groups; however, significantly more for the lung cancer group ($p < 0.001$) followed by the COPD group ($p < 0.01$) when compared to the healthy control group. The baseline DNA damage in PBL of both healthy individuals and asthma patients showed no significant difference.

The CBMN assay

Whole blood was used for the CBMN assay. After stimulating lymphocytes to proliferate, they were treated with 0.1, 0.2, 0.5, and 1 µg/ml GO NMs. Asthma, COPD, and lung cancer patients (asthma, COPD, and lung cancer group) as well as healthy people (control group) provided the blood. Seven cytogenetic damage biomarkers were scored: nuclear buds in

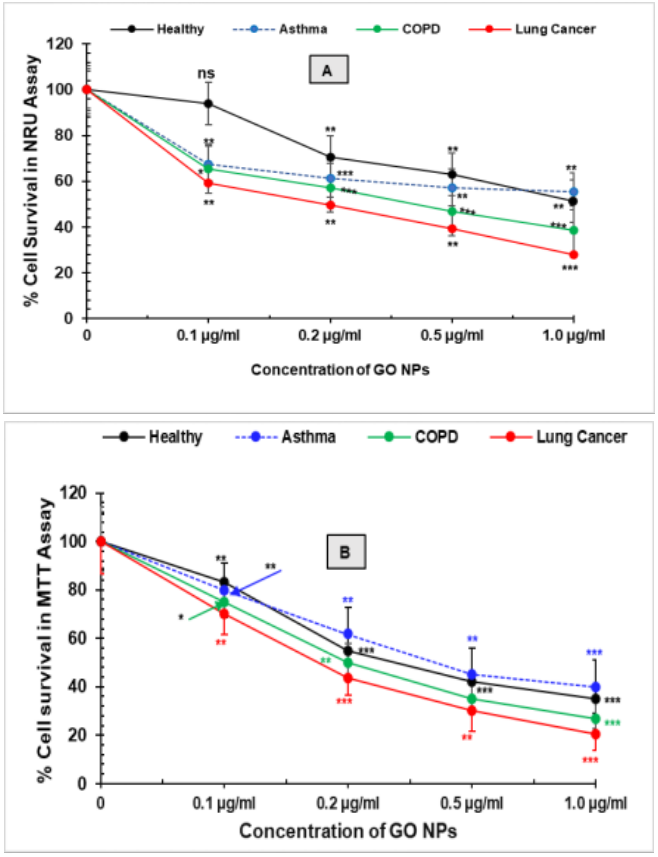

Figure 2: Cytotoxicity of GO (15-20 sheets) in peripheral human lymphocytes after 24 h treatment with different concentrations of GO (0.1, 0.2, 0.5 and 1 µg/ml). The mitochondrial activities were assessed with NRU and MTT assays. The percentage (%) of cell survival of treated lymphocytes was compared with untreated lymphocytes (0 µg/ml: negative control = 100%) in healthy control individuals and pulmonary asthma, COPD, and lung cancer patients. The values represent the mean ± SEM of three independent experiments (n=3). * $p < 0.05$; ** $p < 0.01$; *** $p < 0.001$; ns = not statistically different. Bars indicate standard errors

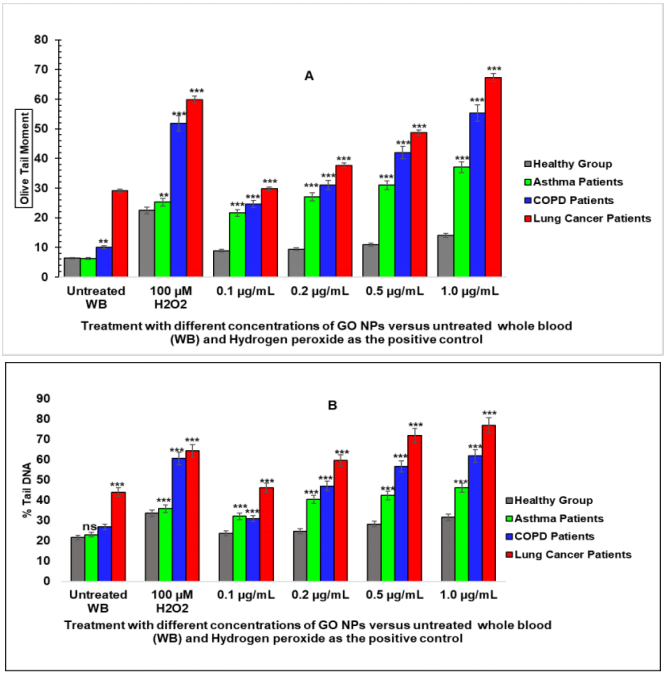

Figure 3: DNA damage in human white blood cells from healthy individuals and patients with asthma, COPD, and lung cancer following 30 min exposure to graphene oxide (GO; 15–20 sheets) at 0.1, 0.2, 0.5, and 1.0 µg/ml, or to 100 µM hydrogen peroxide (H_2O_2) as a positive control. (A) Olive Tail Moment (OTM). (B) Percentage of DNA in comet tail (% Tail DNA). Data represent mean ± SEM from 20 independent Comet assay experiments per treatment group (n = 80 assays total). *p < 0.05; **p < 0.01; ***p < 0.001; ns = not statistically significant.

BiNC (BiNBUD), nucleoplasmic bridges (NPB), mono-, bi-, and multinucleated cells (MonoNC, BiNC & MultiNC), the nuclear division index (NDI), and the frequency of micronuclei in BiNC (BiMNi). Table 6 displays the results for healthy individuals in the control group, the asthma group, the COPD group, and the lung cancer group, respectively.

Mononucleated cells: From 38.12 ± 1.10% for the lowest concentration of 0.1 µg/ml to 24.52 ± 0.63% for the highest GO concentration of 1 µg/ml, the percentage of MonoNC for the control group dropped significantly ($p < 0.001$) in a concentration-dependent manner. The three patient groups also experienced this significant decrease ($p < 0.001$): the asthma group went from 35.20 ± 0.81% to 25.16 ± 0.79%, the COPD group went from 33.12 ± 0.55% to 21.52 ± 0.55%, and the lung cancer group went from 32.24 ± 1.80% to 15.56 ± 1.31%. Therefore, when compared to the healthy control group, the induction of MonoNC was lowest in cancer patients, followed by patients with COPD and asthma.

Binucleated cells: BiNC increased significantly ($p < 0.001$) in a concentration-dependent manner following GO NMs treatment. In particular, the percentage of BiNC (%BiNC) for the healthy control group rose dramatically from 61.16 ± 1.11% for the lowest concentration to 73.52 ± 0.26% for the highest GO concentration. The three patient groups all showed the same pattern of significant increase ($p < 0.001$): the lung cancer group increased from 66.16 ± 1.64% to 80.04 ± 1.26%, the COPD group increased from 65.72 ± 0.52% to 75.84 ± 0.66%, and the asthma group increased from 63.84 ± 0.88% to 72.24 ± 0.72%. When compared to the healthy negative control, the PBL from patients with lung cancer had the highest induction of BiNC, followed by those from patients with COPD and asthma.

Multinucleated cells: Polynuclear cells with three or four nuclei per cell (Ben-Ze'ev and Raz 1981) were assessed after exposure of PBL to GO NMs and the frequency of these induced MultiNC was recorded. For the healthy negative control, the percentage of MultiNC (%MultiNC) significantly increased ($p < 0.001$) with increasing GO concentrations from 1.44 ± 0.21% for the lowest concentration to 4.47 ± 0.41% for the highest concentration. For the asthma group significant numbers of MultiNC were induced from concentrations higher than 0.2 µg/ml. %MultiNC from 1.92 ± 0.27% to 5.20 ± 0.44% were observed. For the COPD group, the lowest concentration of 0.1 µg/ml significantly increased ($p < 0.001$) the percentage of MultiNC from 2.32 ± 0.15% to 2.64 ± 0.16% while doubling the concentration to 0.2 µg/ml resulted in a significant decrease to 2.16 ± 0.10% ($p < 0.001$) possibly due to aggregation of GO particles. Then up to 1 µg/ml, the proportions of %MultiNC increased significantly ($p < 0.001$) to 4.40 ± 0.31% and 5.28 ± 0.74%, respectively. For the lung cancer group, a significant increase was seen ($p < 0.001$) at concentrations higher than 0.2 µg/ml from 3.20 ± 0.42% to 8.80±0.68%, respectively. In summary, the highest induction of MultiNC was observed in the lung cancer group followed by the COPD and asthma groups when compared to the healthy negative control.

Nuclear Division index (NDI)

The NDI is a biomarker of cell proliferation and mitogenic response in the presence of cytotoxic agents (Ionescu et al.

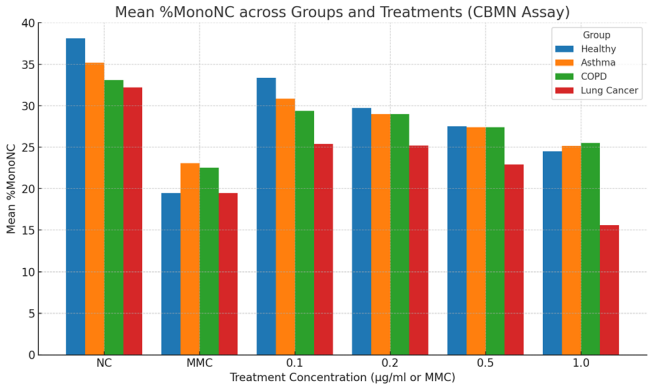

Figure 4: Mean values of various biomarkers of cytogenetic damage in PBL from the healthy control group, asthma group, COPD group and lung cancer group after treatment with graphene oxide (GO) using the CBMN assay (n = 5). DNA damage events were scored binucleated cells (BiNC) and mononucleated cells (MonoNC). MNi induction was statistically significant at 1 µg/ml ($p < 0.05$). Abbreviations: MMC = mitomycin C, MultiNC = multinucleated cells, NDI = nuclear division index, MNi = micronuclei, NPBs = nucleoplasmic bridges and BUDs = nuclear buds.

2011), and its values increased significantly ($p < 0.001$) with increasing GO concentrations (0.1, 0.2, 0.5, and 1 µg/ml) in the healthy control group from 1.63 ± 0.01 to 1.79 ± 0.00 for the highest dose, and in the asthma group from 1.66 ± 0.01 to 1.77 ± 0.01 for the highest dose. The NDI was calculated using Michael Fenck's method, which uses the following formula: where M1 = MonoNC; M2 = BiNC; and N = the total number of viable cells scored (1,000) per concentration (Heshmati et al. 2018). The results for the lung cancer group were similar to those for the COPD group, with a significant increase ($p < 0.001$) observed for all concentration points from 1.69 ± 0.02 to 1.89 ± 0.01 for the highest concentration. The slight fluctuations may be due to GO NMs forming aggregates during incubation because there was no agitation during the incubation period.

Frequencies of induced MNi: According to Podrimaj-Bytyqi et al. (2018), the quantity of induced MNi and other cytogenetic characteristics have been employed as biomarkers (Table 6) of genome instability that contributes to the development of specific cancer forms, including urethral carcinoma. Micronuclei per 1,000 scored binucleated cells (BiMNi) or mononucleated cells (MonoMNi) were used to measure the mean frequencies of induced MNi following treatment with 0.1 and 0.2 µg/ml of GO, respectively, there was a substantial drop in the induced BiMNi in the healthy control group from 1.80 ± 0.66 to 0.80 ± 0.37 and 1.00 ± 0.32 ($p < 0.001$). At doses of 0.5 and 1 µg/ml, the results peaked once more at 3.00 ± 0.71 and 2.80 ± 0.66. At dosages of 0.1 and 0.2 µg/ml of GO, the number of induced MNi for the asthma group dropped from 2.40 ± 0.98 to 1.80 ± 0.66 per 1,000 BiNC, respectively, a significant decrease ($p < 0.001$). However, the mean values of induced BiMNi increased significantly ($p < 0.001$) to 5.20 ± 0.80 and 5.80 ± 1.24, respectively, following exposure to 0.5 and 10 µg/ml of GO.BiMNi induction for the COPD group decreased from 3.80 ± 80 to 3.20 ± 0.58 ($p < 0.001$) after PBL treatment with 0.1 µg/ml of GO. However, more BiMNi was substantially induced ($p < 0.001$) after treatments with 0.2, 0.5, and 1 µg/ml, yielding rates of 5.60 ± 1.03, 5.80 ± 1.46, and 6.00 ± 0.45 per 1,000 BiNC, respectively. Significant ($p < 0.001$) concentration-dependent increases in induced BiMNi were seen for the lung cancer group at all doses of GO NMs, ranging from 3.40 ± 0.51 to 9.40 ± 0.51 for the highest dose.

Chromosome Instability Parameters (NPBs, NBUDs, and MonoMNi)

Chromosomal instability parameters such as nucleoplasmic bridges (NPBs) and nuclear buds (NBUDs) as well as MonoMNi frequencies are used to assess different types of induced cytogenetic damage and were scored in the CBMN assay (Table 6). They are some of the biomarkers of cancer progression and are applied in both cancer diagnosis, prognosis, and pharmacotherapeutic outcomes (Vargas-Rondon et al. 2018).

Healthy Control Group: After treatment with 0.1, 0.2 and 1 µg/ml a small induction of NPBs in binucleated cells (BiNPBs) were observed; for the highest concentration a significant induction of BiNPBs ($p < 0.001$) was observed at 0.60 ± 0.24 per 1,000 BiNC. The highest concentration of GO also significantly induced ($p < 0.001$) BUDs in binucleated cells (BiNBUDs) at a frequency of 0.40 ± 0.24 per 1,000 BiNC. With increasing GO concentrations an increasing number of MNi in mononucleated cells (MonoMNi) were observed. At the highest concentration of 1 µg/ml the frequency of MonoMNi significantly increased ($p < 0.001$) from 0.40 ± 0.24 to 2.60 ± 0.93 per 1,000 MonoNC (extrapolated from raw numbers).

PATIENTS WITH LUNG DISEASES

Asthma Patients: BiNPBs were not induced in PBL treated with 0.1 µg/ml of GO; however, NPBs were significantly ($p < 0.001$) induced in BiNC at treatment concentrations of 0.2, 0.5, and 1 µg/ml. At the maximum GO concentration, 1.20 ± 0.58 per 1,000 BiNC was obtained. Additionally, BiNBUDs increased significantly ($p < 0.001$) from 0.40 ± 0.24 to 1.40 ± 0.60 per 1,000 BiNC at the highest concentration. Following treatment with 0.1, 0.2, 0.5, and 1 µg/ml of GO NMs, the frequencies of the MonoMNi likewise considerably ($p < 0.001$) increased from 1.00 ± 0.32 to 5.20 ± 0.97 per 1,000 MonoNC (extrapolated).

COPD Patients: BiNPBs were only slightly induced in COPD patients' exposed PBL. Significant induction of 0.60 ± 0.24 per 1,000 BiNC was observed at the maximum GO concentration ($p < 0.001$). BiNBUDs and MonoMNi were both inducted in exposed PBL: at the highest GO concentration, there was a substantial ($p < 0.001$) induction of 1.40 ± 0.40 per 1,000 BiNC and 3.20 ± 1.11 per 1,000 (extrapolated) MonoNC, respectively.

Lung Cancer Patients: In untreated PBL, there were 2.00 ± 0.63 BiNPBs for every 1,000 BiNC. PBL exposed to GO (0.1, 0.2, 0.5, and 1 µg/ml) on the other hand, had considerably reduced ($p < 0.001$) BiNPB numbers, ranging from 0.20 ± 0.20 to 1.00 ± 0.45, respectively. For the highest GO dose, BiBUDs were likewise significantly induced ($p < 0.001$) to 1.00 ± 0.32; no BiBUDs were observed in the negative control. At the maximum GO dose of 1 µg/ml, MNi in 1,000 extrapolated mononucleated cells was considerably elevated ($p < 0.001$), rising from untreated control levels of 2.80 ± 0.66 to 7.40 ± 0.51.

Confounding Factors

Eighty people in all, fifty-five percent men and forty-five percent women, were chosen at random to donate blood for the study. Age and lack of cigarette smoking history were not regarded as confounding factors in healthy individuals: 100% of participants had never smoked, and 95% of participants were under 60. Confounding variables including age and cigarette smoking, however, may have affected the outcomes for individuals in the asthma group: Sixty-five percent were

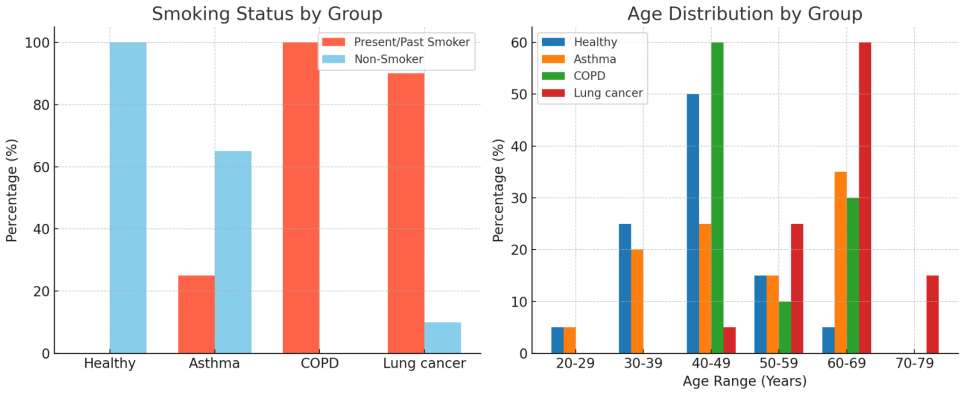

Figure 5: Confounding factors within the blood donors.

under 60 and 25 percent had a history of cigarette smoking. Sixty-five percent of patients in the COPD group were younger than 60, and all participants had a history of smoking. Cigarette smoking caused confusing effects for 90% of patients in the lung cancer group and age (30% under 60 years of age).

Discussion

As the use of nanoparticles grows, it is crucial to thoroughly characterize them in vitro in order to ascertain their physicochemical characteristics, including lateral size and surface charge. These properties have been connected to toxicity, especially for nanomaterials like graphene oxide (GO) (Ou et al., 2016). Compared to scanning electron microscopy (SEM) or transmission electron microscopy (TEM), dynamic light scattering (DLS) yielded larger mean particle size estimates in this investigation. When compared to analyses of dried samples using TEM and SEM, this disparity most likely results from the measurement conditions: DLS evaluates the Brownian motion of particles in aqueous suspension at a specific temperature (Stetefeld et al., 2016), and water molecules intercalating into GO sheets can artificially inflate particle size measurements (Song et al., 2014).

The electrostatic surface charge of particles in dispersion, known as the zeta potential (ZP), which offers information on the stability of nanoparticles and possible cellular uptake, was evaluated using a Zetasizer Nano ZS (Malvern Instruments, UK) (Clogston & Patri, 2011). GO nanoparticles showed a net-negative charge because of their surface chemistry, which included hydroxyl (-OH), carboxyl/ketone (C=O), epoxy/alkoxy (C–O), and aromatic (C=C) groups. This study recorded a ZP value of –23 ± 2 mV (Song et al., 2014). GO's amphiphilic nature (lipophilic and hydrophilic qualities) and potent van der Waals attractions encourage agglomeration in spite of its moderate ZP (Yan & Chou, 2010; Kim et al., 2012). Our observed values indicated that the GO suspension was sufficiently stable, even though ZP values near ±30 mV generally indicate good dispersion stability (Mittal et al., 2017).

DLS is frequently used to size nanoparticles, although it is less accurate for materials that are very polydisperse, such as multi-layered graphene oxide (15–20 sheets). In these situations, measurements may be skewed due to light scattering from bigger particles overshadowing smaller particles (Powers et al., 2006; Filipe et al., 2010; Bhattacharjee, 2016). Furthermore, serum proteins can create a "protein corona" on nanoparticles, increasing measured sizes and producing false positives, and DLS is unable to discriminate between particles of different compositions (Hondow et al., 2012; Barbero et al., 2017).

I used TEM and SEM to get around these restrictions. Because of its shorter electron wavelengths, TEM provides higher resolution (Winey et al., 2014). However, it has significant disadvantages, such as the inability to analyze single samples, the possibility of agglomeration during air-drying, and sample damage from the electron beam, which makes it inappropriate for thermolabile materials (Hondow et al., 2012; Wills et al., 2017). Moreover, TEM pictures show 2D agglomerate cross-sections, which might not accurately depict 3D particle shape. To maintain nanoparticles in a nearly native condition and prevent agglomeration during imaging, other techniques such cryogenic plunge-freezing and digital Fourier microscopy (DFM) have been proposed (Wills et al., 2017).

I chose the MTT and neutral red uptake (NRU) tests for cytotoxicity assessment because of their excellent sensitivity and dependability. NRU examines lysosomal function, whereas MTT evaluates mitochondrial enzyme activity (Mossman, 1983a; Stone et al., 2009). Although NRU is typically faster, more sensitive, and less expensive, both are frequently employed in drug screening (Repetto et al., 2008; Hansen & Bross, 2010). In contrast to doses up to 1 µg/ml, which resulted in irreversible cell death, GO at 0.1–0.2 µg/ml produced genotoxicity without cytotoxicity in our investigation.

However, in vitro assay cell lines may have chromosomal defects and mutations, which makes them unreliable indicators of human responses in vivo (Ding et al., 2014). Due in part to

variations in GO surface chemistry, impurities, and synthesis techniques, previous research on GO's hemolytic and thrombotoxic effects has shown contradictory findings (Sasidharan et al., 2012; Liao et al., 2011; Singh et al., 2011, 2012). Variations in assay trends point to potential interactions between GO and assay reagents, especially the MTT dye, although our use of commercial GO helped preserve consistency (Liao et al., 2011).

It is true that MTT can be chemically reduced by carbon nanomaterials, which would cause cell viability estimations to be inflated (Monteiro-Riviere & Inman, 2006). Mn^{2+} and Fe^{2+} ions, which are impurities from the Hummers' process, might intensify cytotoxic and genotoxic effects (Liu et al., 2013; Stephenson et al., 2013; Stéfani et al., 2011). Other reagents, including WST-8, might be better to lessen assay interference (Wu et al., 2015; Ou et al., 2016). Furthermore, cell viability at the start of the assay is crucial since prolonged incubation might result in false-positive or misleading results due to natural apoptosis or necrosis (Ding et al., 2014).

Confounding factors may have also played important roles in the significant cytotoxicity responses observed in both COPD and lung cancer patients since 100% of individuals with COPD and lung cancer were smokers, with some of them smoking up to 30 cigarettes per day.

According to comet assay data, DNA damage clearly increased as graphene oxide (GO) concentrations rose. This effect was driven by both the study participants' pathological states and GO levels. Higher GO concentrations can encourage particle agglomeration, which decreases direct contact with cells, therefore this tendency might not always be consistent. Interestingly, when compared to lymphocytes from COPD patients and healthy control subjects (treated or untreated, NC), lung cancer patients' lymphocytes showed the most DNA damage. Patients with lung cancer are particularly vulnerable because of their diminished capacity to repair damaged DNA, which leads to genetic abnormalities and the advancement of the disease (Orlow et al., 2015). To put it simply, their DNA is more vulnerable to genotoxic substances.

On the other hand, the amounts of DNA damage in the lymphocytes of asthmatic patients and healthy people were almost the same. This was corroborated by Stephenson et al. (2013), who used the alkaline Comet test to show that Mn^{2+} and Fe^{2+} ions might cause DNA damage. These results highlight how crucial it is to evaluate possible contaminants in GO, especially in materials that are purchased commercially, and, where practical, measure their concentrations before carrying out thorough cytotoxicity and genotoxicity analyses.

The CBMN assay was used to measure chromosomal instability and cytogenetic damage in cells that had only completed one nuclear division. When cytochalasin B prevented cytokinesis, a cytoplasmic division, at the conclusion of mitosis (nuclear division), binucleated cells (BiNC) were created; cells that do not divide, for instance, as a result of exposure to GO, could still be identified as mononucleated cells (MonoNC). Chromosome segments that failed to segregate with the mitotic spindle were evaluated in both BiNC and MonoNC (Kirsch-Volders and Fenech 2001; Fenech 2002). Lung cancer is characterized by the accumulation of cytogenetic damage markers, such as the frequency of MNi, which vary according to the clinical status of the individual (El-Zein et al. 2008).

The genotoxicity of GO NMs (15–20 sheets) and the need for additional investigation are highlighted by our findings. On the one hand, lymphocytes from both the cancer and COPD groups showed noticeably higher levels of CBMN endpoints, which is a good indication that GONPs could be a great option for anti-cancer drug delivery (Ma et al. 2015) and that GO could be utilized for COPD nanotherapeutics (Seshadri and Ramamurthi 2018). Lymphocytes from patients with lung cancer ($n = 5$; $p < 0.001$) had a considerably higher induction of MNi, a biomarker for cytogenetic damage, than lymphocytes from patients with COPD.According to Albertini et al. (2000), MNi are chromatin-containing entities that can represent whole missegregation or chromosomal fragments. Accordingly, GO may be categorized as both an aneugen that results in missegregated chromosomes when it interferes with the spindle apparatus during mitosis and a clastogen that causes chromosomal breaks when it interacts with DNA directly or indirectly (Bignold 2009). Chromosome fragments that missegregate during the anaphase of mitosis are caused by GO's capacity to cause DNA DSBs. As a result, the CBMN assay shows the production of MNi. After the daughter nuclei formed, cytokinesis was inhibited by adding cytochalasin B 44 hours after the blood culture began (20 hours after GO and MMC treatments).

Since blood lymphocytes must pass through areas of increased inflammation or oxidative stress, the high proliferation rate of the affected cells and the inflammatory changes in the microenvironment leading up to the development of chronic pathological conditions may be the cause of the significant induction of cytostatic event parameters (lower levels of MonoNC, and high levels of MultiNC and BiNC) seen frequently in lymphocytes from lung cancer and COPD patients rather than in those from asthma patients or healthy individuals (Dai et al. 2017; Anderson et al. 2019). Our findings are in line with other studies that demonstrated the potent anticancer effects of GO NMs (Szmidt et al. 2019). Compared to those from asthma patients and healthy people, cultured lymphocytes from patients with lung cancer and COPD had a greater rise in both the proportion of BiNC and the frequency of MNi in BiNC (BiMNi). According to El-Zein et al. (2008), elevated levels of BiMNi are a biomarker of cancer susceptibility and may be used to predict the development of cancer in healthy people who are vulnerable to DNA damage. According to earlier studies, the average NDI value was substantially lower

in patients with colorectal cancer (CRC) than in patients with normal colonoscopy (1.57 vs. 1.73) and in patients with lung cancer than in the negative controls (1.52 vs. 2.08, p<0.001) (El-Zein et al. 2008). (Ionescu and others, 2011). The group found that the cut-off value that indicated adenomas or carcinomas was 1.5 – that means the lower the NDI value, the higher the likelihood of cancer in this case

Their results, however, run counter to our findings because our NDI values rose as the concentration of GO nanoparticles increased. Oxaliplatin (OXP) is one drug that is known to function differently. According to Alotaibi et al. (2017), the high values of multinucleated cells in OXP patients caused their NDI values to be greater than those of the untreated PBL from a healthy negative control individual (1.82 vs. 1.73). The CBMN assay results readily concur with the concentration-dependent increases in GO nanomaterial cytotoxicity that we previously demonstrated using the MTT and NRU assays, as well as in the genotoxicity (DNA damage) investigations using the alkaline Comet assay.

During our tests, the CBMN assay showed certain limitations, despite its widespread use in genetic toxicology studies (İpek et al. 2017). It was unsuitable for field research when quick findings are needed since, first of all, it was quite time-consuming and could result in more human error and inter-laboratory disparities (Radack et al. 1995; Fenech et al. 2003). Second, although being employed at low concentrations that shouldn't cause major harm, the spindle inhibitor cytochalasin B may work in concert or as an additive with the therapy chemical to cause further DNA damage or alter the cells' rates of proliferation (Albertini et al. 2000). Additionally, a lengthy culture period is a significant factor that may cause MNi frequencies to be overestimated, most likely as a result of delayed cell division in the already damaged cells. Age and smoking history may be complicating factors in the notable disparities in cytogenetic responses between blood lymphocytes from patients and those from healthy people.

Conclusion

In conclusion, our results are based on lymphocytes that were chosen as somatic cell surrogates and subjected to GO NMs. According to our research, GO NMs may damage healthy cells in COPD and lung patients if they are produced pharmaceutically as nanocarriers for the delivery of drugs that target COPD and lung cancer cells. Concerns about workplace exposure and the paradigm shift into drug delivery applications once the nanomaterials have completed their work at the cancer target sites are raised by the in vitro demonstration of varying degrees of cytotoxicity, genotoxicity (DNA damage), and chromosome aberrations by peripheral blood leukocytes from healthy individuals who were assumed to be immunocompetent. The data acquired for our study also contributes to the body of knowledge about the genotoxicity and cytotoxicity of the various GO NM types. These results clearly demonstrate that more comprehensive genotoxicity studies of GO (15–20 sheets) must be carried out both in vitro and in vivo in order to develop safer nanomaterials. Understanding the molecular mechanism by which GO NMs cause DNA damage is crucial, as is resolving conflicting genotoxicity data on different GO types and sizes (Liu et al. 2013; Wu et al. 2015).

References

1. Albertini, R. J., Anderson, D., Douglas, G. R., Hagmar, L., Hemminki, K., Merlo, F., Natarajan, A. T., Norppa, H., Shuker, D. E. G., Tice, R., Waters, M. D. and Aitio, A. (2000) IPCS guidelines for the monitoring of genotoxic effects of carcinogens in humans. International Programme on Chemical Safety. *Mutation Research-Reviews in Mutation Research* 463 (2), 111-172.
2. Amadi, E. E. (2019). Effects of Graphene Oxide in vitro on DNA Damage in Human Whole Blood and Peripheral Blood Lymphocytes from Healthy Individuals and Pulmonary Disease Patients: Asthma, COPD, and Lung Cancer [Doctoral dissertation, University of Bradford, UK]. BradScholars. Available at: https://bradscholars.brad.ac.uk/handle/10454/18685
3. Anderson, D., Najafzadeh, M., Scally, A., Jacob, B., Griffith, J., Chaha, R., Linforth, R., Soussaline, M. and Soussaline, F. (2019) Using a Modified Lymphocyte Genome Sensitivity (LGS) test or TumorScan test to detect cancer at an early stage in each individual. *FASEB Bioadv* 1 (1), 32-39.
4. Aslantürk, Ö. S. (2017) In Vitro Cytotoxicity and Cell Viability Assays: Principles, Advantages, and Disadvantages. *IntechOpen*.
5. Azqueta, A. and Dusinska, M. (2015) The use of the comet assay for the evaluation of the genotoxicity of nanomaterials. *Frontiers in Genetics* 6.
6. Barbero, F., Russo, L., Vitali, M., Piella, J., Salvo, I., Borrajo, M. L., Busquets-Fité, M., Grandori, R., Bastús, N. G., Casals, E. and Puntes, V. (2017) Formation of the Protein Corona: The Interface between Nanoparticles and the Immune System. *Seminars in Immunology* 34, 52-60.
7. Ben-Ze'ev, A. and Raz, A. (1981) Multinucleation and inhibition of cytokinesis in suspended cells: reversal upon reattachment to a substrate. *Cell* 26 (1 Pt 1), 107-15.
8. Bhattacharjee, S. (2016) DLS and zeta potential – What they are and what they are not? *Journal of Controlled Release* 235, 337-351.
9. Bignold, L. P. (2009) Mechanisms of clastogen-induced chromosomal aberrations: A critical review and description of a model based on failures of tethering of DNA strand ends to strand-breaking enzymes. *Mutation Research-Reviews in Mutation Research* 681 (2), 271-298.
10. Böyum, A. (1968) Separation of leukocytes from blood and bone marrow. Introduction. *Scand J Clin Lab Invest Suppl.* 97 (7).
11. Clogston, J. D. and Patri, A. K. (2011) Zeta potential measurement. *Methods Mol Biol* 697, 63-70.
12. Dai, J., Yang, P., Cox, A. and Jiang, G. (2017) Lung cancer and chronic obstructive pulmonary disease: From a clinical perspective. *Oncotarget* 8 (11), 18513.

13. Daniels, T. R., Delgado, T., Helguera, G. and Penichet, M. L. (2006) The transferrin receptor part II: Targeted delivery of therapeutic agents into cancer cells. *Clinical Immunology* 121 (2), 159-176.
14. Dinauer, N., Balthasar, S., Weber, C., Kreuter, J., Langer, K. and von Briesen, H. (2005) Selective targeting of antibody-conjugated nanoparticles to leukemic cells and primary T-lymphocytes. *Biomaterials* 26 (29), 5898-5906.
15. Ding, Z., Zhang, Z., Ma, H. and Chen, Y. (2014) In vitro hemocompatibility and toxic mechanism of graphene oxide on human peripheral blood T lymphocytes and serum albumin. *ACS applied materials & interfaces* 6 (22), 19797-19807.
16. El-Zein, R. A., Fenech, M., Lopez, M. S., Spitz, M. R. and Etzel, C. J. (2008) Cytokinesis-Blocked Micronucleus Cytome Assay Biomarkers Identify Lung Cancer Cases Amongst Smokers. *Cancer Epidemiol Biomarkers Prev.* 17 (5), 1111-119.
17. Fenech, M. (2002) Chromosomal biomarkers of genomic instability relevant to cancer. *Drug Discovery Today* 7 (Generic), 1128-1137.
18. Fenech, M. (2007) Cytokinesis-block Micronucleus Cytome Assay. *Nature Protocols* 2 (5), 1084-1104.
19. Fenech, M., Bonassi, S., Turner, J., Lando, C., Ceppi, M., Chang, W. P., Holland, N., Kirsch-Volders, M., Zeiger, E., Bigatti, M. P., Bolognesi, C., Cao, J., De Luca, G., Di Giorgio, M., Ferguson, L. R., Fucic, A., Lima, O. G., Hadjidekova, V. V., Hrelia, P., Jaworska, A., Joksic, G., Krishnaja, A. P., Lee, T.-K., Martelli, A., McKay, M. J., Migliore, L., Mirkova, E., Müller, W.-U., Odagiri, Y., Orsiere, T., Scarfi, M. R., Silva, M. J., Sofuni, T., Suralles, J., Trenta, G., Vorobtsova, I., Vral, A. and Zijno, A. (2003) Intra- and inter-laboratory variation in the scoring of micronuclei and nucleoplasmic bridges in binucleated human lymphocytes: Results of an international slide-scoring exercise by the HUMN project. *Mut.Res.-Genetic Toxicology and Environmental Mutagenesis* 534 (1), 45-64.
20. Filipe, V., Hawe, A. and Jiskoot, W. (2010) Critical Evaluation of Nanoparticle Tracking Analysis (NTA) by NanoSight for the Measurement of Nanoparticles and Protein Aggregates. *Pharmaceutical Research* 27 (5), 796-810.
21. Gerashchenko, B. I. (2017) On scoring cytokinetic and binucleated cells. *Cytometry A* 91 (7), 655-656.
22. Hansen, J. and Bross, P. (2010) A cellular viability assay to monitor drug toxicity. *Methods Mol Biol.* 648, 303-11.
23. Heshmati, M., Hajibabae, S. and Barikrow, N. (2018) Genotoxicity and Cytotoxicity Assessment of Graphene Oxide Nanosheets on HT29 Cells. *Journal of Kermanshah University of Medical Sciences* 22 (1).
24. Hondow, N., Brydson, R., Wang, P., Holton, M. D., Brown, M. R., Rees, P., Summers, H. D. and Brown, A. (2012) Quantitative characterization of nanoparticle agglomeration within biological media. *Journal of Nanoparticle Research* 14 (7), 1-15.
25. Ionescu, M. E., Ciocirlan, M., Becheanu, G., Nicolaie, T., Ditescu, C., Teiusanu, A. G., Gologan, S. I., Arbanas, T. and Diculescu, M. M. (2011) Nuclear Division Index may Predict Neoplastic Colorectal Lesions. *Maedica (Buchar)* 6 (3), 173-178.
26. Karbaschi, M. and Cooke, M. S. (2014) Novel method for the high-throughput processing of slides for the comet assay. *Scientific reports* 4, 7200.
27. Kim, J., Cote, L. J. and Huang, J. (2012) Two Dimensional Soft material: new faces of Graphene Oxide. *Accounts of chemical research* 45 (8), 1356-1364.
28. Kirsch-Volders, M. and Fenech, M. (2001) Inclusion of micronuclei in non-divided mononuclear lymphocytes and necrosis/apoptosis may provide a more comprehensive cytokinesis block micronucleus assay for biomonitoring purposes. *Mutagenesis* 16 (1), 51-58.
29. Liao, K.-H., Lin, Y.-S., Macosko, C. W. and Haynes, C. L. (2011) Cytotoxicity of graphene oxide and graphene in human erythrocytes and skin fibroblasts. *ACS applied materials & interfaces* 3 (7), 2607-2615.
30. Liu, J., Cui, L. and Losic, D. (2013) Graphene and graphene oxide as new nanocarriers for drug delivery applications. *Acta biomaterialia* 9 (12), 9243-9257.
31. Ma, N., Zhang, P., Zhang, B., Liu, J., Li, Z. and Luan, Y. (2015) Green fabricated reduced graphene oxide: evaluation of its application as nano-carrier for pH-sensitive drug delivery. *International Journal of Pharmaceutics* 496 (2), 984-992.
32. Mittal, S., Sharma, P. K., Tiwari, R., Rayavarapu, R. G., Shankar, J., Chauhan, L. K. S. and Pandey, A. K. (2017) Impaired lysosomal activity mediated autophagic flux disruption by graphite carbon nanofibers induce apoptosis in human lung epithelial cells through oxidative stress and energetic impairment. *Particle and fibre toxicology* 14 (1), 15-25.
33. Mohamadi, S. and Hamidi, M. (2017) The new nanocarriers based on graphene and graphene oxide for drug delivery applications. *Nanostructures for Drug Delivery: Micro and Nano Technologies.* Online: 107-147.
34. Monteiro-Riviere, N. A. and Inman, A. O. (2006) Challenges for assessing carbon nanomaterial toxicity to the skin. *Carbon* 44 (6), 1070-1078.
35. Mossman, T. (1983a) Rapid colorimetric assay for cellular growth and survival: application to proliferation and cytotoxicity assays. *Journal of Immunological Methods* 65, 55-63.
36. Mossman, T. (1983b) Rapid colorimetric assay for cellular growth and survival: Application to proliferation and cytotoxicity assays. *Journal of Immunological Methods* 65 (1-2), 55-63.
37. Nasongkla, N., Shuai, X., Ai, H., Weinberg, B. D., Pink, J., Boothman, D. A. and Gao, J. (2004) cRGD-functionalized polymer micelles for targeted doxorubicin delivery. *Angewandte Chemie - International Edition* 43 (46), 6323-6327.
38. OECD (2016) Test No. 489: In Vivo Mammalian Alkaline Comet Assay. *https://www.oecd-ilibrary.org/docserver/9789264264885-en.pdf?expires=1543337897&id=id&accname=guest&checksum=6DC18CD4BF2F11016194FC0BB182F0D5* Accessed 27th Nov 2018
39. Orlow, I., Park, B. J., Mujumdar, U., Patel, H., P., S.-L., Clas, B., R., D., Flores, R., Bains, M., Rizk, N., Dominguez, G., Jani, J., Berwick, M., Begg, C., Kris, M. and Rusch, V. (2015) DNA Damage and Repair Capacity in Lung Cancer Patients: Prediction of Multiple Primary Tumors. *J Clin Oncol.* 26 (21), 3560-3566.
40. Ou, L., Song, B., Liang, H., Liu, J., Feng, X., Deng, B., Sun, T. and Shao, L. (2016) Toxicity of graphene-family nanoparticles: a general review of the origins and mechanisms. *Particle and fibre toxicology* 13 (1), 57.
41. Parveen, S., Misra, R. and Sahoo, S. (2012) Nanoparticles: a boon to drug delivery, therapeutics, diagnostics and imaging. *Nanomedicine* 8 (2), 147-166.

42. Podrimaj-Bytyqi, A., Borovečki, A., Selimi, Q., Manxhuka-Kerliu, S., Gashi, G. and Elezaj, I. R. (2018) The frequencies of micronuclei, nucleoplasmic bridges and nuclear buds as biomarkers of genomic instability in patients with urothelial cell carcinoma. *Scientific Reports* 8 (1), 17873.
43. Powers, K. W., Brown, S. C., Krishna, V. B., Wasdo, S. C., Moudgil, B. M. and Roberts, S. M. (2006) Research strategies for safety evaluation of nanomaterials. Part VI. Characterization of nanoscale particles for toxicological evaluation. *Toxicological sciences : an official journal of the Society of Toxicology* 90 (2), 296-303.
44. Radack, K. L., Pinney, S. M. and Livingston, G. K. (1995) Sources of variability in the human lymphocyte micronucleus assay: a population-based study. *Environ Mol Mutagen* 26 (1), 26-36.
45. Rebuttini, V., Fazio, E., Santangelo, S., Neri, F., Caputo, G., Martin, C., Brousse, T., Favier , F. and Pinna, N. (2015) Chemical Modification of Graphene Oxide through Diazonium Chemistry and Its Influence on the Structure–Property Relationships of Graphene Oxide–Iron Oxide Nanocomposites. *Chemistry – A European Journal* 21 (35), 12465-12474.
46. Repetto, G., del Peso, A. and Zurita, J. L. (2008) Neutral red uptake assay for the estimation of cell viability/cytotoxicity. *Nature Protocols* 3 (7), 1125-1131.
47. Sasidharan, A., Panchakarla, L. S., Sadanandan, A. R., Ashokan, A., Chandran, P., Girish, C. M., Menon, D., Nair, S. V., Rao, C. N. R. and Koyakutty, M. (2012) Hemocompatibility and macrophage response of pristine and functionalized graphene. *Small (Weinheim an der Bergstrasse, Germany)* 8 (8), 1251-1263.
48. Seshadri, D. R. and Ramamurthi, A. (2018) Nanotherapeutics to Modulate the Compromised Micro-Environment for Lung Cancers and Chronic Obstructive Pulmonary Disease. *Frontiers in pharmacology* 9, 759.
49. Singh, S. K., Singh, M. K., Kulkarni, P. P., Sonkar, V. K., Grácio, J. J. A. and Dash, D. (2012) Amine-Modified Graphene: Thrombo-Protective Safer Alternative to Graphene Oxide for Biomedical Applications. *ACS Nano* 6 (3), 2731-2740.
50. Singh, S. K., Singh, M. K., Nayak, M. K., Kumari, S., Shrivastava, S., Grácio, J. J. A. and Dash, D. (2011) Thrombus Inducing Property of Atomically Thin Graphene Oxide Sheets. *ACS Nano* 5 (6), 4987-4996.
51. Song, J., Wang, X. and Chang, C.-T. (2014) Preparation and Characterization of Graphene Oxide. *Journal of Nanomaterials* 2014, 1-6.
52. STEMCELL Technologies (2017) *Lymphoprep Density Gradient Medium for the Isolation of mononuclear cells*. 2017. Online: STEMCELL Technologies Canada Inc. *https://cdn.stemcell.com/media/files/pis/29283-PIS_1_3_0.pdf?_ga=2.11894386.777538854.1552913845-1383156917.1552913845*
53. Stephenson, A. P., Schneider, J. A., Nelson, B. C., Atha, D. H., Jain, A., Soliman, K. F. A., Aschner, M., Mazzio, E. and Renee Reams, R. (2013) Manganese-induced oxidative DNA damage in neuronal SH-SY5Y cells: Attenuation of thymine base lesions by glutathione and N-acetylcysteine. *Toxicology Letters* 218 (3), 299-307.
54. Stetefeld, J., McKenna, S. A. and Patel, T. R. (2016) Dynamic light scattering: a practical guide and applications in biomedical sciences. *Biophys Rev* 8 (4), 409-427.
55. Stone, V., Johnston, H. and Schins, R. (2009) Development of in vitro systems for nanotoxicology: methodological considerations. *Crit Rev Toxicol.* 39 (7), 613-26.
56. Stéfani, D., Paula, A. J., Vaz, B. G., Silva, R. A., Andrade, N. F., Justo, G. Z., Ferreira, C. V., Filho, A. G. S., Eberlin, M. N. and Alves, O. L. (2011) Structural and proactive safety aspects of oxidation debris from multiwalled carbon nanotubes. *Journal of Hazardous Materials* 189 (1), 391-396.
57. Sun, X., Liu, Z., Welsher, K., Robinson, J. T., Goodwin, A., Zaric, S. and Dai, H. (2008) Nano-graphene oxide for cellular imaging and drug delivery. *Nano Res.* 1 (3), 203-212.
58. Szmidt, M., Stankiewicz, A., UrbaAska, K., Jaworski, S., Kutwin, M., Wierzbicki, M., Grodzik, M., BurzyAska, B., Gora, M., Chwalibog, A. and Sawosz, E. (2019) Graphene oxide down-regulates genes of the oxidative phosphorylation complexes in a glioblastoma. *BMC Molecular Biology* 20 (1), 1-9.
59. Tice, R. R., Agurell, A., D., Burlinson, B., Hartmann, A., Kobayashi, H., Miyamae, Y., Rojas, E., Ryu, J.-C. and Sasaki, Y. F. (2000) Single Cell Gel/Comet Assay: Guidelines for In Vitro and In Vivo Genetic Toxicology Testing. *Environmental and Molecular Mutagenesis* 35, 206-221.
60. U.S. National Library of Medicine (2019) *Lung Cancer.* Online: *https://ghr.nlm.nih.gov/condition/lung-cancer* Accessed 20 Mar 2019.
61. Vargas-Rondon, Villegas, V. E. and Rondon-Lagos, M. (2018) The Role of Chromosomal Instability in Cancer and Therapeutic Responses. *Cancers (Based)* 10 (4).
62. Wang, K., Ruan, J., Song, H., Zhang, J., Wo, Y., Guo, S. and Cui, D. (2011a) Biocompatibility of Graphene Oxide. *Nanoscale Research Letters* 6 (1), 1-8.
63. Wang, Y., Wang, J., Li, J., Li, Z. and Lin, Y. (2011b) Graphene and graphene oxide: biofunctionalization and applications in biotechnology. *Trends in Biotechnology* 29 (5), 205-212.
64. Wills, J. W., Summers, H. D., Hondow, N., Sooresh, A., Meissner, K. E., White, P. A., Rees, P., Brown, A. and Doak, S. H. (2017) Characterizing Nanoparticles in Biological Matrices: Tipping Points in Agglomeration State and Cellular Delivery In Vitro. *ACS Nano* 11 (12), 11986-12000.
65. Winey, M., Meehl, J. B., O'Toole, E. T. and Giddings, J. T. H. (2014) Conventional transmission electron microscopy. *Molecular biology of the cell* 25 (3), 319-323.
66. Wu, S.-Y., An, S. S. A. and Hulme, J. (2015) Current applications of graphene oxide in nanomedicine. *International journal of nanomedicine* 10 Spec Iss, 9-24.
67. Yang, K., Zhang, S., Zhang, G., Sun, X., Lee, S.-T. and Liu, Z. (2010) Graphene in mice: Ultrahigh in vivo tumor uptake and efficient photothermal therapy. *Nano Letters* 10 (9), 3318-3323.
68. Zhao, X., Yang, L., Li, X., Jia, X., Liu, L., Zeng, J., Guo, J. and Liu, P. (2015) Functionalized graphene oxide nanoparticles for cancer cell-specific delivery of antitumor drug. *Bioconjugate chemistry* 26 (1), 128-136.
69. İpek, E., Ermiş, E., Uysal, H., Kızılet, H., Demirelli, S., Yıldırım, E., Ünver, S., Demir, B. and Kızılet, N. (2017) The relationship of micronucleus frequency and nuclear division index with coronary artery disease SYNTAX and Gensini scores. *Anatol J Cardiol* 17 (6), 483-489.